Coordination motifs and large-scale structural organization in atomic clusters

Yang, Zhu; Tang, Lei-Han

Published in:
Physical Review B

DOI:
10.1103/PhysRevB.79.045402

Published: 05/01/2009

Document Version:
Peer reviewed version

Coordination motifs and large-scale structural organization in atomic clusters

Zhu Yang and Lei-Han Tang
Department of Physics, Hong Kong Baptist University, Kowloon Tong, Hong Kong SAR, China
(Dated: September 29, 2008)

The structure of nanoclusters is complex to describe due to their noncrystallinity, yet bonding and packing constraints often limit the local atomic arrangements to only a few types. A computational scheme is presented to extract coordination motifs from sample atomic configurations. The method is based on a clustering analysis of multipole moments for atoms in the first coodination shell. We demonstrate the power of the method in capturing large-scale structural properties by scanning the ground state of the Lennard-Jones and C_{60} clusters collected at the Cambridge Cluster Database.

PACS numbers: 61.46.-w, 36.40.Mr, 61.43.-j, 64.70.Nd

Nanoscale atomic clusters have attracted a great deal of attention in recent years due to their promising applications in catalysis, photonics, and bioimaging.[1–3] The functionality of these clusters is controlled by their structure, which may assume a variety of forms as a result of the generally complex energy landscape governing the low energy cluster conformations.[4] The atomic arrangements in these clusters generally do not follow the crystal structure of the corresponding bulk material, but may nevertheless possess certain regularities. Suitable representation of these structures, particularly for small and medium sized clusters, is important in the study of mechanisms underlying their thermodynamic stability and functionality.

Traditionally, atomic clusters of high point symmetry are described in terms of the five Platonic solids and their truncated polyhedra.[4,5] Starting from, say, a 13-atom core as illustrated in Fig. 1, successive layers of atoms can be added to produce clusters of "magic size" which feature prominently in spectroscopic measurements. Two particularly well-known series are the Mackay icosahedra[6] (MIC) that grow from Fig. 1(c) and the Marks decahedra[7] (MD) that grow from Fig. 1(d). Noble-gas nanoclusters follow the Mackay icosahedra series up to a few thousand atoms before switching to the Marks decahedra series.[8] Both types of clusters can be viewed as multiply twined particles that take advantage of the low energy surfaces of the constituting face-centered-cubic (fcc) grains. At even larger sizes, accumulation of strain in the particle drives a transition to the single crystal structure, although the size at which this transition takes place is still debated.[9]

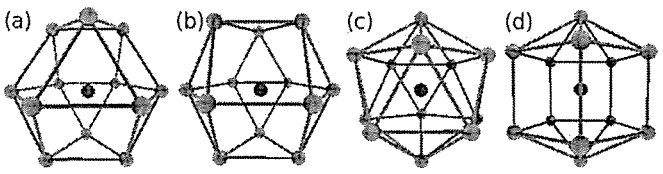

FIG. 1: The first coordination shell at coordination number 12. (a) face-centered-cubic (fcc); (b) hexagonal-close-packed (hcp); (c) icosahedral (ico); (d) decahedral (dec).

Real structures often contain defects and imperfections as compared to the ideal ones.[10] Recently, Polak *et al.* investigated medium-sized Lennard-Jones (LJ) clusters obtained in Monte Carlo simulations at low temperatures.[11,12] They proposed a scheme to describe the interior structure of an atomic cluster in terms of the four "coordination polyhedra" of Fig. 1. Indeed, when atoms with a particular type of coordination are displayed, large-scale features such as cubic domains or polyicosahedral grains become evident. The visualization scheme has been successful in describing key features of structure evolution during cooling runs, and in cluster growth starting from a seed crystallite. The insights generated from such studies can aid experimental designs aimed at producing a particular class of nanoclusters.

In this paper, we extend Polak's work to construct a systematic and robust computational framework for coordination analysis and large-scale structure identification. This is necessary as the local atomic structures often contain distortions or even belong to unknown categories. Given a set of atomic coordinates, we first compute the radial distribution function to determine a suitable cutoff distance for the first coordination shell. We then parametrize the coordination shell configuration of each interior atom using the multipole moments Q_l of the shell atoms.[13] The data set is examined for their clustering properties. Each well-defined cluster in the data set represents a re-occuring local structural unit which we call a "coordination motif". Atoms in the same cluster are then assigned the same "type". The scheme allows for fast classification of interior atoms and their local neighborhoods. The geometric properties of individual motifs and their spatial organization provide valuable information for large-scale structure analysis. In particular, the MIC and the MD series each possesses a unique composition profile of the coordination motifs. Hence the motif content alone can be used for accurate structure association.

We illustrate our method in the description of the (putative) ground state of LJ clusters with up to $N = 1610$ atoms, available at the Cambridge Cluster Database (CCD).[14,15] Figure 2(a) shows the radial distribution function obtained from the histogram of pairwise distances $r_{ij} = |\mathbf{r}_i - \mathbf{r}_j|$ for three selected atomic clusters

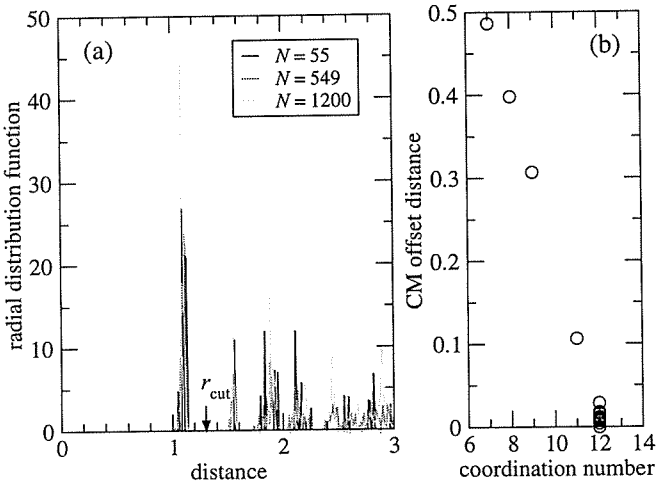

FIG. 2: (Color online) (a) Radial distribution function of LJ clusters at three selected sizes. (b) The distance between the center of mass (CM) of the first coordination shell and the center atom against the coodination number for all atoms in a $N = 549$ cluster. Here $r_{\rm cut} = 1.3$.

at $N = 55, 549$ (complete Mackay icosahedra) and 1200, at a bin size $\Delta r = 0.01$ (in units of the LJ radius σ). In all three cases, there are well-defined distance gaps which allow for unambiguous identification of first and second coordination shells for all atoms in the cluster. The plot suggests a cut-off distance $r_{\rm cut} = 1.3$ for the first coordination shell. To distinguish interior from surface atoms, we compute the offset distance $r_{\rm offset}$ between the center atom and the center of mass (CM) of its first coordination shell. Figure 2(b) shows a scatter plot of $r_{\rm offset}$ against the coordination number for all atoms on the $N = 549$ cluster. The approximately linear behavior of the data indicates that completed shells have 12 atoms.

The 12-atom neighborhoods as shown in Fig. 1 are distinguished from one another by the angular distribution of atoms on the shell. Provided the distance of shell atoms to the center atom falls in a narrow range, the shell configuration is well represented by a density function $\rho(\theta, \phi) = \sum_k \delta(\theta - \theta_k, \phi - \phi_k)$, where (θ_k, ϕ_k) are the polar coordinates of shell atom k with the origin on the center atom. Consider now the "multipole" expansion in the spherical harmonics,

$$\rho(\theta, \phi) = \sum_{l,m} a_{lm} Y_{lm}(\theta, \phi), \qquad (1)$$

where $a_{lm} = \sum_k Y^*_{lm}(\theta_k, \phi_k)$. The multipole moments of the shell configuration are given by,[13]

$$Q_l \equiv \frac{1}{C}\sqrt{\frac{4\pi}{2l+1}\sum_{m=-l}^{l}|a_{lm}|^2} = \sqrt{\frac{4\pi}{2l+1}\sum_{m=-l}^{l}|\overline{Y}^*_{lm}|^2}, \qquad (2)$$

where C is the number of shell atoms, and the overline bar denotes average over the shell. Note that $Q_l = 1$ (all l) if there is only one atom on the shell.

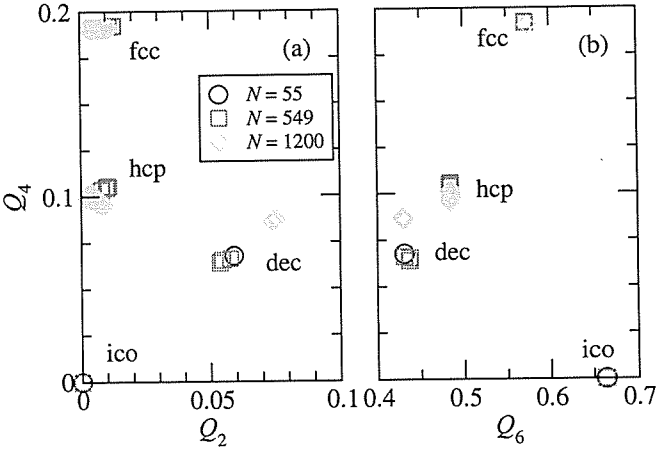

FIG. 3: (Color online) Scatter plot of the multipole moments of interior atoms on the ground state LJ clusters at three different cluster sizes. (a) Q_4 versus Q_2; (b) Q_4 versus Q_6.

In Ref.[11], the moments Q_4 and Q_6 are used to differentiate the four atomic configurations shown in Fig. 1. We propose here a more general approach based on the clustering property of interior atoms in the space spanned by the multipole moments $\{Q_l\}$. Atoms that are close to each other in this representation have very similar neighborhoods. Strong clustering of the data points suggests existence of only a few coordination motifs. Standard clustering methods[16] can then be used to assign coordination motifs to the atoms. On the other hand, weak clustering would imply a more continuous spectrum of local neighborhoods without a clear local structural preference.

Figure 3 shows the multipole moments Q_2, Q_4 and Q_6 for all interior atoms on the ground-state LJ clusters at the three selected sizes. In all cases the data exhibit very strong clustering in a way that corresponds well to the four shell configurations in Fig. 1. The decagonal (dec) motif is the only one that has a sizable Q_2 due to its directionality. This property can be used to distinguish it from the hexagonal-close-packed (hcp) motif which has similar values of Q_4 and Q_6. Splitting of the corresponding cluster suggests that the dec motif is more deformable. The other three motifs are easily distinguishable using Q_4.

Using the moment pair (Q_2, Q_4) as classifier, we computed the composition profile $c_\alpha = N_\alpha/N_{\rm interior}$ of the four coordination motifs for all ground state LJ clusters in the size range $N = 13 - 1610$. Here N_α is the number of α = fcc, hcp, ico, dec atoms in the cluster interior and $N_{\rm interior}$ is the total number of interior atoms. Results are shown in Fig. 4. Each curve gives the percentage of a particular motif in the atomic cluster against the cluster size. As a reference, Table I lists the number of interior atoms of each type for complete Mackay icosahedra and Marks decahedra as a function of the layer number n. Also given are the total number of interior atoms $N_{\rm interior}$ as well as the cluster size N. Using these expressions, we computed the concentration of the fcc

TABLE I: Number of icosahedral (ico), decahedral (dec), hexagonal-close-packed (hcp) and face-centered-cubic (fcc) coordinated atoms in the complete Mackay icosahedra (MIC) and Marks decahedra (MD) series. The total number of completed shells (including surface atoms) is given by n.

	MIC	MD
$N_{\rm ico}$	1	0
$N_{\rm dec}$	$12(n-1)$	$2n-1$
$N_{\rm hcp}$	$15(n-1)(n-2)$	$\frac{5}{2}(n-1)(3n-2)$
$N_{\rm fcc}$	$\frac{10}{3}(n-1)(n-2)(n-3)$	$\frac{5}{6}n(n-1)(4n-5)$
$N_{\rm interior}$	$(2n-1)[\frac{5}{3}n(n-1)+1]$	$\frac{10}{3}n^3-\frac{19}{3}n+4$
N	$(2n+1)[\frac{5}{3}n(n+1)+1]$	$\frac{10}{3}n^3+10n^2+\frac{11}{3}n+1$

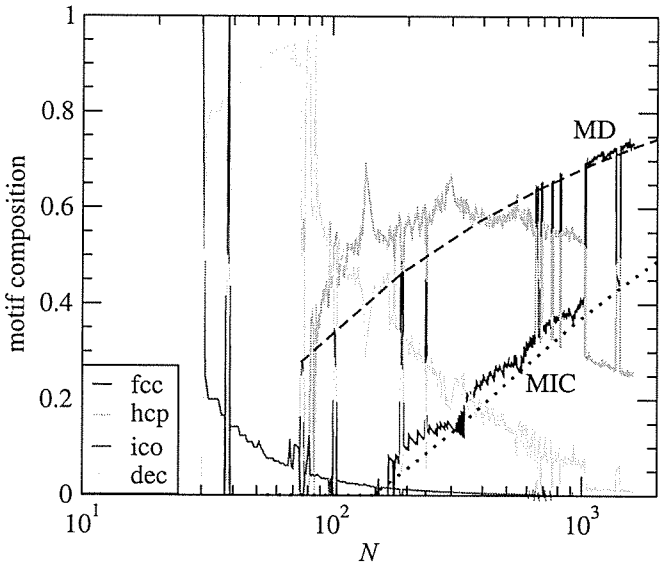

FIG. 4: (Color online) Composition profile of four coordination motifs in the ground state LJ clusters. Dashed and dotted lines give the theoretical values of $c_{\rm fcc}$ for complete Mackay icosahedra and Marks decahedra, respectively.

motif for the two series, as indicated by the dashed and dotted lines in Fig. 4. Some overall trend of structure evolution is evident. Beyond $N = 147$ (three completed shells in an icosahedral structure), the ground state essentially alternates between two structures. The main transition between the icosahedra-dominated regime at smaller sizes to the decahedra-dominated regime at larger sizes takes place at around $N = 1030$, indicated by an upward jump in the $c_{\rm fcc}$ curve (black solid line) on the plot. Windows exist on either side of the transition where the minority series pops in. The physical mechanism behind these transitions, which has to do with the competition between strain and surface energies, has already been discussed extensively in the literature.[17]

The spatial distribution of the coordination motifs offers much valuable information about large-scale structural organization. Figure 5 shows the position of ico (blue), dec (green), and hcp (orange) atoms in the $N =$

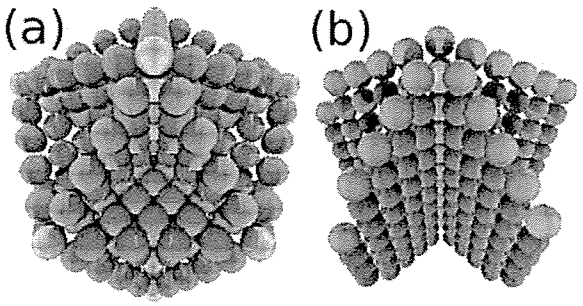

FIG. 5: (Color online) Position of ico (blue), dec (green), and hcp (orange) atoms in the ground state LJ cluster at size (a) $N = 923$ (Mackay icosahedron) and (b) $N = 1103$ (Marks decahedron), showing large-scale structural organization.

923 (MIC) and 1103 (MD) clusters. The icosahedrally coordinated atom is only present at the center of the MIC cluster. The decagonally coordinated atoms are located on the five-fold symmetry axis in both clusters, while the hcp atoms form two-dimensional sheets that separate the fcc grains (not shown) at symmetry related crystallographic orientations.

Clusters of size less than three atomic layers exhibit a greater variety of organizational behavior due to the more subtle and delicate competition among packing, strain, and surface effects. Figure 6 shows the composition profiles in this size range for two representative classes of ground states in the CCD, the LJ clusters discussed above and the C_{60} clusters computed using the Pacheco and Prates-Ramalho potential.[18] Most of the LJ clusters in this size range contain a single icosahedron motif (open blue circle) at the core. Their structure essentially follows that of the Mackay icosahedra series, with modifications close to the surface layer. Notable exceptions are found at $N = 38$ (fcc) and $N = 75 - 77$ (Marks decahedron), where the icosahedron motif is missing. For the C_{60} clusters, the icosahedron core is present only at $N \leq 15$. About one third of the clusters in the size range $31 - 100$ are cubic (i.e., with only fcc and hcp motifs), whereas the rest contain some form of the decahedral structure. It has been suggested that, due to the narrow range of the molecular potential, C_{60} clusters prefer close-packed structures as compared to the LJ clusters.[18,19] This is in good agreement with the much higher percentage of fcc, hcp, and dec motifs in the composition profiles as shown in Fig. 6. We have also examined the different series of the ground state Morse clusters in the CCD that correspond to a broad range of softness of the pair potential.[20] Indeed, as the range of the interaction shortens, a change from the icosahedral to decagonal and cubic structures is observed.

The decahedral motif plays a special role in the large-scale structural organization due to the directionality of the pentagonal symmetry axis. In both the Mackay icosahedra and Marks decahedra series, they stack together to form linear chains to propagate the (local) pentagonal

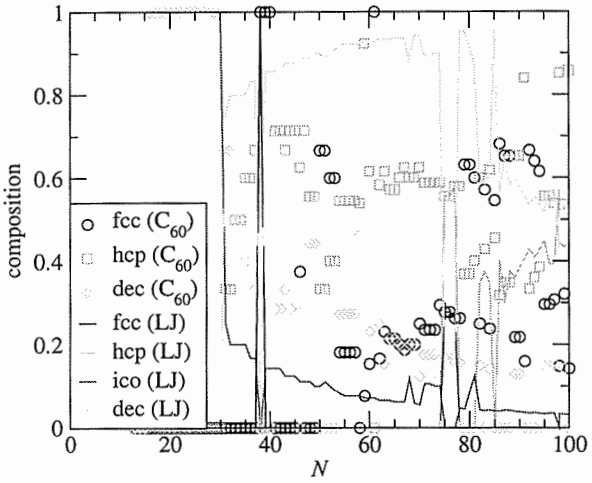

FIG. 6: (Color online) Motif composition profile for Lennard-Jones (LJ) and C_{60} clusters below $N = 100$.

symmetry all the way to the the cluster surface. Two or more pentagonal axes can emanate from an icosahedral motif or an incomplete icosahedron at the surface. The network of decahedral motifs, with information on their orientation, adds a great deal of transparency to the three-dimensional structure of the atomic clusters.

In summary, we have presented a general method to identify re-occuring local structural units in an atomic cluster without prior information. The structural units, taken here to be atoms on the first coordination shell, are represented by a set of multipole moments whose clustering properties form the basis for robust and efficient classification schemes. Applying the scheme to the ground state of the LJ and C_{60} clusters, we reconfirmed that the fcc, hcp, ico and dec motifs provide a complete list of the 12-atom neighborhood for all interior atoms. For the LJ clusters, the motif compositions show a systematic dependence on cluster size, in agreement with the existing understanding on the structure evolution of these clusters. Large-scale structural organization are readily revealed when interior atoms are displayed according to their type, significantly reducing the level of complexity in structure representation. We believe that the approach represents an important step in the development of coarse-grained models that focus on the interplay between geometry and energetics to elucidate the equilibrium and kinetic properties of medium-sized atomic clusters at low temperatures.

We wish to thank Dr. X.-G. Shao for providing the LJ cluster coordinates in the size range 1001-1610. This work was supported by the Research Grants Council of the HKSAR through grant HKBU 2020/04P.

[1] G. Schmid, M. Bäumle, M. Geerkens, I. Heim, C. Osemann, and T. Sawitowski, Chem. Soc. Rev. **28**, 179 (1999).
[2] F. Baletto and R. Ferrando, Rev. Mod. Phys. **77**, 371 (2005).
[3] M. Walter, J. Akola, O. Lopez-Acevedo, P. D. Jadzinsky, G. Calero, C. J. Ackerson, R. L. Whetten, H. Grönbeck, and H. Häkkinen, Proc. Natl. Acad. Sci. **105**, 9157 (2008).
[4] D. J. Wales, *Energy Landscapes*, Cambridge Univ. Press, Cambridge, 2003.
[5] T. P. Martin, Phys. Rep. **273**, 199 (1996).
[6] A. L. Mackay, Acta Cryst. **15**, 916 (1962).
[7] L. D. Marks, Phil. Mag. A **49**, 81 (1984).
[8] V. Kiryukhin, E. P. Bernard, V. V. Khmelenko, R. E. Boltnev, N. V. Krainyukova, and D. M. Lee, Phys. Rev. Lett. **98**, 195506 (2007).
[9] N. V. Krainyukova, Eur. Phys. J. D **43**, 45 (2007).
[10] B. W. van de Waal, G. Torchet, and M.-F. de Feraudy, Chem. Phys. Lett. **331**, 57 (2000).
[11] W. Polak and A. Patrykiejew, Phys. Rev. B **67**, 115402 (2003).
[12] W. Polak, Phys. Rev. E **77**, 031404 (2008).
[13] P. J. Steinhardt, D. R. Nelson, and M. Ronchetti, Phys. Rev. B **28**, 784 (1983).
[14] http://www-wales.ch.cam.ac.uk/CCD.html.
[15] X. Shao, Y. Xiang, and W. Cai, J. Phys. Chem. A **109**, 5193 (2005).
[16] J. Kogan, *Introduction to Clustering Large and High-Dimensional Data*, Cambridge Univ. Press, Cambridge, 2007.
[17] J. P. K. Doye and F. Calvo, J. Chem. Phys. **116**, 8307 (2002).
[18] J. P. K. Doye, D. J. Wales, W. Branz, and F. Calvo, Phys Rev. B **64**, 235409 (2001).
[19] J. P. K. Doye and D. J. Wales, Chem. Phys. Lett. **247**, 339 (1995).
[20] J. P. K. Doye and D. J. Wales, J. Phys. B **29**, 4859 (1996).